J. Anat. (1999) **195**, pp. 429–437, with 3 figures Printed in the United Kingdom

Application of the fractionator and vertical slices to estimate total capillary length in skeletal muscle

EMILIO ARTACHO-PÉRULA[1], RAFAEL ROLDÁN-VILLALOBOS[1] AND LUIS M. CRUZ-ORIVE[2]

[1] *Department of Morphological Sciences* (*Section of Histology*), *School of Medicine*, *University of Córdoba*, *and*
[2] *Department of Mathematics*, *Statistics and Computation*, *Faculty of Sciences*, *University of Cantabria*, *Santander*, *Spain*

(*Accepted 1 June 1999*)

ABSTRACT

A new stereological method is proposed which combines vertical slice projections with the fractionator to estimate the total capillary length in a skeletal muscle. The method was demonstrated on the soleus muscle of a Wistar rat. The implementation required capillary highlighting, tissue sampling, and data acquisition in the form of intersection counts between capillary projections and cycloid test lines. The capillaries were demonstrated using vascular perfusion (with gelatine) of the hind leg of the rat. The sampling procedure followed the fractionator design, namely a multistage systematic sampling design with a known sampling fraction at each stage. To make the design unbiased, vertical slices were used; for efficiency, the vertical axis was chosen parallel to the main axis of the muscle. As prescribed to avoid bias, the cycloid test lines were superimposed on the slice projections, viewed under the light microscope, with their minor axes normal to the vertical axis. The estimation precision was compared for different sampling and subsampling fractions. The proposed method was globally highly efficient, unbiased, and easy to implement.

Key words: Vasculature; stereology.

INTRODUCTION

The capillary supply of skeletal muscle has been widely studied under normal and experimental conditions (Plyley et al. 1976, 1998; Myrhage, 1977; Appell, 1980; Aquin & Banchero, 1981; Hoppeler et al. 1981; Poole & Mathieu-Costello, 1989; Artacho-Pérula et al. 1990; Snyder, 1995; Kano et al. 1997). To quantify the capillary network is important for understanding different functional and metabolic features of skeletal muscle.

In normal subjects, the microvascular arrangement of skeletal muscle varies between and within muscles, species, and even in relation to the degree of muscle activity. Several methods have been published to estimate muscle capillarity (Mathieu-Costello, 1993). Quantification of capillaries in skeletal muscle was, at least initially, based on the model of Krogh (1919) who assumed that the capillaries were straight and unbranched pipes running parallel to the muscle fibres. However, it is known that capillaries are branched and exhibit tortuosity to various degrees.

Often, muscle capillarity is quantified on transverse sections of skeletal muscle. The directly observed numerical density of capillary profiles and the capillary-to-fibre profile ratio have been the most common descriptors of muscle capillarity (Sillau & Banchero, 1977; Ripoll et al. 1979; Artacho-Pérula et al. 1990, 1991). The reciprocal of the latter ratio (sharing factor) has also been used (Plyley & Groom, 1975). Basic structural descriptors of the capillary network are, however, the length density (Hoppeler, 1984) and the surface density of capillaries regarded as 3-dimensional tubular structures. Since anisotropy is present in skeletal muscle capillaries, the method proposed by Mathieu et al. (1983) and Cruz-Orive et al. (1985) requires transverse and longitudinal sections to quantify the degree of capillary orientation and to estimate the ratio of capillary length to fibre volume (Mathieu-Costello, 1993); this method is based on a particular model for the directional distribution of the capillaries, however, and it is therefore not design unbiased.

The vertical sections design (Baddeley et al. 1986) is

Correspondence to Dr E. Artacho-Pérula, Department of Morphological Sciences (Section of Histology), School of Medicine, University of Córdoba. Avda. Menéndez Pidal, s/n. E-14071 Córdoba (Spain). Tel: +34 957 218261; fax: +34 957 218246; e-mail: cm1arpee@lucano.uco.es

a genuine unbiased design to estimate surface area, whereas the vertical slices design (Gokhale, 1990) is unbiased to estimate the length of curvilinear features. The latter method has been successfully applied to estimate capillary length in rat heart (Batra et al. 1995), and in skeletal muscle (Artacho-Pérula & Roldán-Villalobos, 1995*a*, *b*) as well as microvessel length in cerebral cortex (McMillan et al. 1994).

The purpose of this paper is twofold. First, to present a new combination of the fractionator (hitherto used only to estimate cell number) and vertical slices to estimate the finite length of a curvilinear structure contained in a bounded object. And second, to demonstrate the method and to explore its precision on the capillary bed of the rat soleus muscle.

MATERIALS AND METHODS

Material and its preparation to demonstrate capillaries

The material chosen to illustrate the methods was the soleus muscle of a 9-mo-old male Wistar rat of 480 g body weight. The animal was subjected to i.p. anaesthesia with 50 mg/kg of pentobarbital in Ringer solution after halothane induction. Vascular perfusion was carried out after laparotomy and local application of lidocaine. The protocol comprised the following stages: (1) location of the blood vessels (aorta, vena cava and iliacs); (2) tying the aorta and iliac arteries; (3) insertion of a cannula in the left iliac artery; (4) opening the left iliac vein; (5) perfusion through the cannula in the following steps: (5.1) rinsing with Ringer solution pH 7.4, 310 mOsm plus heparin 20000 u/l plus papaverine 0.25% for 5 min at a pressure of 100 mmHg and 37 °C; (5.2) addition of 3% glutaraldehyde at pH 7.4; (5.3) additional Ringer rinse; and (5.4) perfusion with gelatine for 10 min at 37 °C. Subsequently, the left soleus muscle was dissected, removed from the leg, and weighed. The target parameter was the total length of capillaries in this muscle.

Stereology

The fractionator (Gundersen, 1986) is an unbiased and efficient method to estimate any additive geometric quantity—such as number, length, surface area and volume—defined on a bounded object. Hitherto the fractionator has apparently been applied only to estimate the number of separate features in an organ, such as neurons, lymph valves and inhaled particles in lung, etc. For further details and references, see Howard & Reed (1998). In this paper we concentrate on the estimation of the total length L of a finite aggregate of curvilinear or tubular features (skeletal muscle capillaries in our example) in a bounded object (the left soleus muscle of a Wistar rat). The idea was hinted at in Cruz-Orive & Howard (1991), but not developed further. Very recently the fractionator has been proposed by Larsen et al. (1998) to estimate length in combination with optical scanning of sectioning planes in isotropic directions. In this paper we combine the fractionator with a vertical slices design.

Here we briefly describe the principle; the details of its practical implementation, with reference to Figure 1, are given in the next subsection.

The fractionator is multistage systematic sampling of fragments from a solid object, with a known sampling fraction at each stage. In the first stage the object is split into a few fragments (slices, logs, or indeed pieces of arbitrary size and shape, as convenient) and every f_1th fragment is chosen with a uniform random start among $\{1, 2, \ldots, f_1\}$. If we knew the total length L_1 of capillaries in the chosen fragments, then $f_1 \times L_1$ would be an unbiased estimator of the total length L. Usually the direct estimation of L_1 will not be feasible at the first stage. In a second stage, the fragments chosen at the first stage are further split into pieces; every f_2th piece is chosen with a fresh random start among $\{1, 2, \ldots, f_2\}$, and so forth until we consider that the estimation of the total length L_k of curvilinear features in the pieces sampled at the kth stage, say, is feasible. Only the integers $f_1, f_2, \ldots, f_k$, which are called the sampling periods (namely the reciprocals of the corresponding sampling fractions) need to be remembered. An unbiased estimator of the total L in the intact object is:

$$\text{est}\, L = f_1 \times f_2 \times \ldots \times f_k \times L_k, \text{cm} \qquad (1)$$

Unbiasedness requires only strict adherence to the choice of a uniform random start at each sampling stage; object shape, cutting directions, etc. do not affect the unbiasedness of est L in Eq. (1). The unbiased estimation of the last stage length L_k, however, requires either isotropic plane probes (Larsen et al. 1998) or vertical slices (Gokhale, 1990; for an abridged description, see Cruz-Orive. 1997, subsection 6.2). For this reason the whole splitting design has to be conceived so that the final sample consists of properly oriented fragments. In our design (Fig. 1) the final sample consisted of vertical slices for light microscopy, with the capillaries easily identifiable after projection.

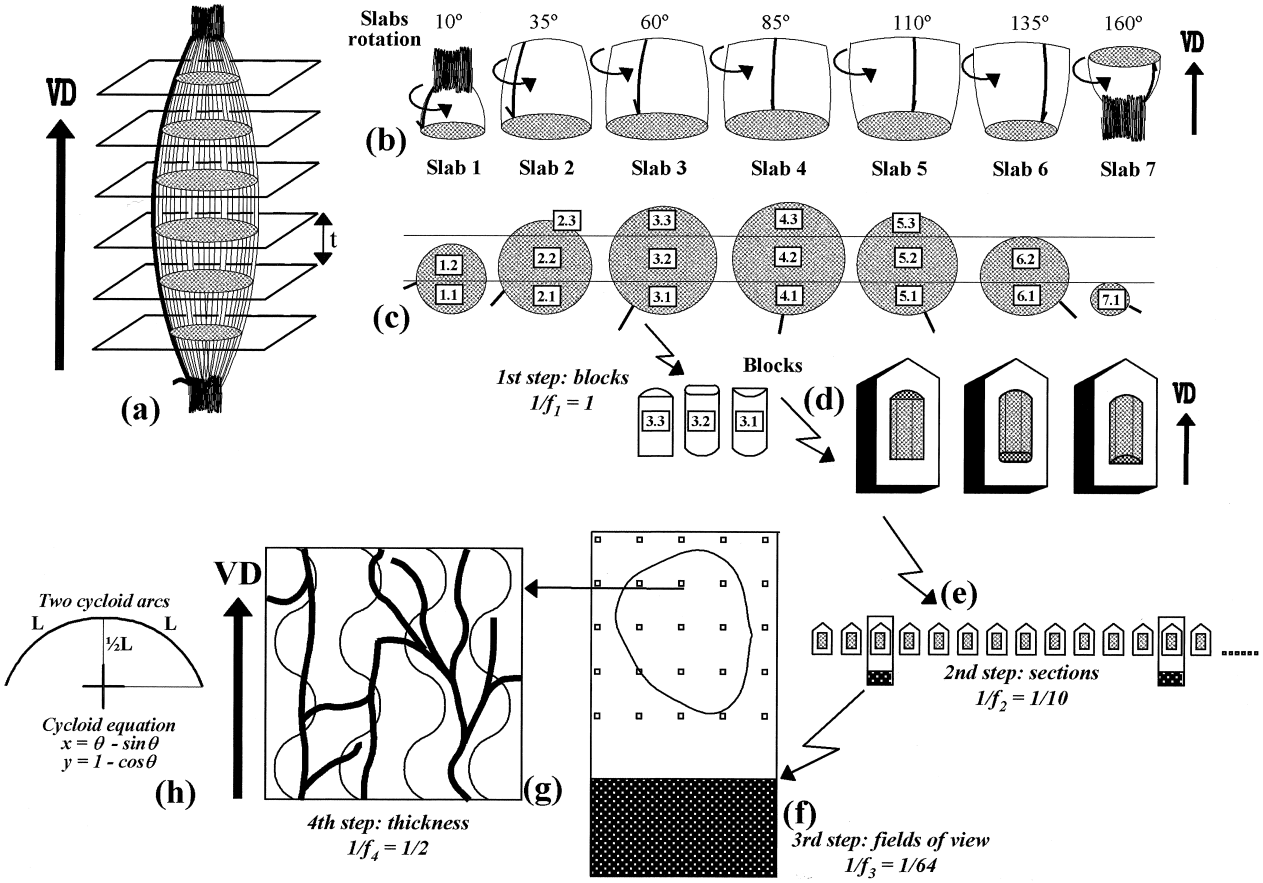

Fig. 1. Illustration of the fractionator design with vertical slices to estimate total capillary length in a rat soleus muscle. (*a*) The complete muscle was first split (in a nonrandom manner) into seven slabs about 4 mm thick; VD, vertical direction. The thick longitudinal curve at the left hand side border of the muscle represents the common origin of angles for subsequent rotation of the slabs. (*b*) The slabs were systematically rotated about the common VD with a period of 180°/7 = 25° and a random start (10°) between 0° and 25°. (*c*) The rotated slabs (viewed from above in the figure) were thereby split into vertical slices or blocks; 17 blocks were thus obtained. No subsampling was performed yet, that is, the first subsampling period was $f_1 = 1$. (*d*) Each block was embedded in glycol-methacrylate, aligning the vertical direction of the muscle with the major axis of the inclusion mould. (*e*) Each block was exhaustively sectioned in LM vertical slices or thick sections of 50 μm nominal thickness, parallel to the previously cut artificial vertical faces. Every 10th section was subsampled ($f_2 = 10$) with a random start between 1 and 10. (*f*) Each subsampled vertical section was subsampled under the LM by systematic quadrats or fields of view ($f_3 = 64$). (*g*) Each quadrat was scanned inside the section by parallel optical planes by a total depth of 25 μm (thus, $f_4 = 50/25 = 2$). A test system consisting of vertical cycloid test lines was superimposed, always in focus; the observed intersections between the cycloids and the capillary projections (thick curves) were counted whenever the latter appeared sharp. (*h*) The length of an arc of a cycloid curve is 4 times the length of its minor principal axis.

Consider a set of vertical slices of a suitable thickness, containing curvilinear features of total length L_k. Project the contents of each slice orthogonally onto an observation plane parallel to the slice faces. On the resulting image, superimpose a system of cycloid test lines with the major axes parallel to the vertical direction. Count the intersections between the cycloids and the feature projections in all slices. In the absence of masking, an unbiased estimator of L_k is:

$$\text{est}\, L_k = 2 \times \tfrac{a}{l} \times I, \text{cm} \qquad (2)$$

where a/l is the test area per test line length for the cycloid test system used, and I represents the total number of intersections counted in all slices (Cruz-Orive & Howard, 1991). Replacing L_k in the right hand side of Eq. (1) with the preceding estimator, we obtain our final estimator of the total length of curvilinear features in the object, namely,

$$\text{est}\, L = f_1 \times f_2 \times \ldots \times f_k \times 2 \times \tfrac{a}{l} \times I, \text{cm} \qquad (3)$$

Practical implementation

The sampling procedure was an adaptation of the foregoing principles, and it ran according to the following steps.

1. Given the shape of the muscle (Fig. 1*a*) it was convenient and efficient to choose the vertical axis parallel to the longitudinal axis of the muscle.

2. The muscle was cut transversely into 'logs' —called 'slabs' hereafter—of ~4 mm thickness (7 slabs were obtained, see Fig. 1*b*). A tissue slicer with

razor blades, similar to that illustrated in Baddeley et al. (1986, fig. 6) was used. No subsampling was performed at this stage.

3. Each slab was systematically rotated around the vertical axis by an angle of $180°/7 \sim 25°$ with a random start in the interval (0°, 25°). The random choice was 10°, and therefore the slabs were rotated 10°, 35°, 60°, 85°, 110°, 135° and 160°, respectively, from the original alignment. Parallel vertical cuts on the whole set of rotated slabs now produced 17 thick vertical slices—called 'blocks' hereafter—of up to 2 mm thickness (Fig. 1*c*). In further routine studies a systematic subsample of blocks could be drawn already at this stage with period $f_1 = 2$, for instance. In this first methodological study we decided to keep all blocks, i.e. we adopted $f_1 = 1$.

4. All vertical blocks were infiltrated with glycol-methacrylate (Historesin), see Figure 1*d*. For posterior identification, care was taken to orient the vertical direction, i.e. the longitudinal axis of the muscle, along the major axis of the inclusion mould. All blocks were exhaustively sectioned (parallel to the vertical direction) with a Reichert-Jung microtome into slices of 50 μm nominal thickness. Hereafter we shall refer to the latter as 'sections'.

5. At this stage we subsampled every 10th section (i.e. the second sampling period was $f_2 = 10$), with a random start given by a random number among $\{1, 2, \ldots, 10\}$, in our study this number was 3 (Fig. 1*e*), hence we sampled the 3rd, 13th, 23rd, …, etc. sections until the list of sections was exhausted. A total of 133 sections of 50 μm nominal thickness were thereby obtained. The actual section thickness was measured in every 10th section (i.e. in 13 sections) with the aid of the microcator (see (6–iv) below) and it yielded a mean thickness of 49.5 μm, (S.D. = 3.2 μm). We adopted a mean thickness of 50 μm in our calculations.

6. The sections were stained with haematoxylin-eosin and subsampled by systematic fields of view or quadrats, with a subsampling area fraction of 1/64, namely $f_3 = 64$, see Figure 1*f*. This, and subsequent tasks, were carried out with the aid of a modified Olympus BH-2 microscope equipped with (i) a set of motors attached to the specimen stage for stepwise, predetermined movements in the x and y-axes; (ii) a Hitachi colour camera for the visualisation of the image on a monitor; (iii) an 'object rotator' on the specimen stage, to enable the slide to be rotated at will while keeping the stage fixed; and (iv) an electronic microcator (Heidenhain VRZ401) to measure the motion of the microscope stage in the z-axis (with a precision of 0.5 μm).

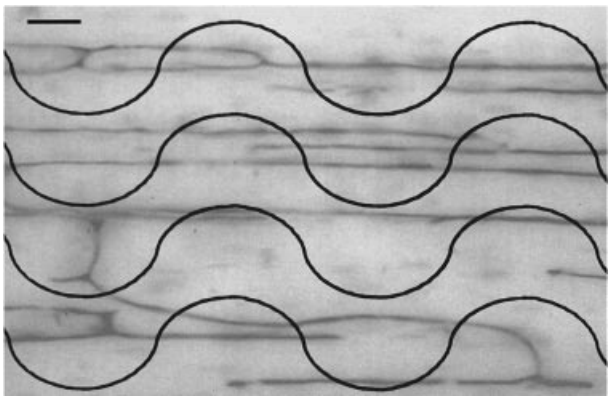

Fig. 2. Total projection of a vertical slice (Fig. 1*g*) of Historesin embedded muscle tissue showing the gelatin perfused capillary network. The projected depth was 25 μm. A portion of the cycloid test system used to estimate capillary length by intersection counting is overlaid with the major principal axes parallel to the vertical direction (Fig. 1*a*), which, for convenience, runs from left to right here. Bar, 25 μm.

7. On each quadrat, a test system of cycloids was superimposed, with the major axes parallel to the vertical direction, as described by the theory (Fig. 2). Proper alignment was achieved with the aid of the object rotator. The test system was always kept in focus. A focal plane was chosen near the upper face of the slice, and the microcator was set to zero there. Subsequently, a depth of 25 μm (measured with the microcator) was scanned inside the slice. Thus the 4th and last sampling period was $f_4 = 2$. As soon as an intersection between a cycloid and the left border of a capillary projection appeared in focus, the intersection was counted. An objective lens of $\times 40$ (NA = 0.65) was used, and the final linear magnification was $\times 1000$. The sum of all intersections over all quadrats and all slices was substituted into the right side of Eq. (3), together with the remaining known constants, to obtain the required estimator of the total capillary length.

Precision

In a study involving 2 or more groups of animals, it is useful to get some idea of the 'error' of est L within animals in order to compare it with the biological variation (Gundersen & Østerby, 1981; Cruz-Orive, 1994). We reconsider this point briefly in the Discussion.

We quantify the precision of the unbiased estimator est L of the unknown capillary length L for a given individual by its coefficient of error:

$$\mathrm{CE}(\mathrm{est}\, L) = \frac{\mathrm{SE}(\mathrm{est}\, L)}{L}. \qquad (4)$$

The fractionator is a very simple method to obtain an efficient and unbiased estimator of a total quantity; however, to predict the corresponding error is a difficult problem because the observations are dependent in a complicated way. Here we apply the error prediction formula of Cruz-Orive (1990) which gives only an approximation but not an unbiased estimator of CE(est L). We describe the necessary steps with reference to the particular design illustrated in Figure 1.

1. Split the 7 slabs into 2 subsets, one consisting of the odd numbered slabs {1, 3, 5, 7}, and the other of the even numbered slabs {2, 4, 6}.

2. Proceed independently for each subset (namely with fresh and independent random numbers), but use the same subsampling periods for each subset (namely the fixed numbers f_1,f_2,f_3,f_4 for blocks, sections, quadrats or fields, and thickness period, respectively). Let I_o, I_e denote the total numbers of intersections (between capillary projections and cycloids, as usual) counted for the odd and the even subsets of slabs, respectively. The final est L is computed via Eq. (6) below with I(cap) replaced by I_o+I_e, and the associated CE is approximated by:

$$\mathrm{CE}(\mathrm{est}\,L) = \frac{1}{\sqrt{3}}\frac{|I_o-I_e|}{I_o+I_e} \tag{5}$$

(Cruz-Orive, 1990).

RESULTS

Total capillary length

The capillary bed in muscle tissue was highlighted qualitatively by the gelatine perfusion method. The presence of some tortuosity meant that the capillaries can in general not be regarded as straight, even in fully extended muscle in situ. The nature of the capillary network, with its many bifurcations and interconnections can be appreciated in Figure 2.

On the quantitative side, the muscle was first split into 7 slabs, and these into 17 blocks, with no subsampling ($f_1 = 1$). The blocks were exhaustively sliced, and the first systematic sample, with period $f_2 = 10$, consisted of 133 slices for light microscopy. In turn, a total of 732 quadrats were subsampled from the sampled slices, with period $f_3 = 64$. The quadrat area was 22560 μm², and the constant a/l of the test system used was 23.5 μm (corrected for magnification). As indicated in step (7) of the *Practical implementation* subsection, for each quadrat intersections were counted by a stepwise scanning of a total depth of 25 μm inside the slice. In Figure 3, top, 6 consecutive steps, 5 μm apart in the z-axis, are illustrated. In Figure 3, bottom, the overall projection of the 25 μm thick portion of the slice at the same site is represented (at a slightly larger magnification). The number of intersections per field ranged between 0 and 46, with an average of 16. Direct application of Eq. (3) yielded:

$$\begin{aligned}\mathrm{est}\,L(\mathrm{cap}) &= f_1\times f_2\times f_3\times f_4\times 2\times(a/l)\times I(\mathrm{cap})\\ &= 1\times 10\times 64\times 2\times 2\times 23.5\ \mu\mathrm{m}\times 11480\\ &= 690.6\times 10^6\ \mu\mathrm{m}\approx 691\ \mathrm{m}.\end{aligned} \tag{6}$$

Assessment of precision

For the complete design described above (Fig. 1) we applied Eq. (5) as explained in Table 1, to obtain CE(est L) ≈ 0.040, namely a 4.0 % error. This design implies exhaustive sampling at the first stage (i.e. all blocks were taken, $f_1 = 1$). The question addressed here is can we predict the CE(est L) for larger sampling periods at one or more stages? This is explored next.

Every other block, ($f_1 = 2$), remaining periods unchanged

The list of the 9 blocks from the odd unnumbered slices is:

{1.1 1.2 | 3.1 3.2 3.3 | 5.1 5.2 5.3 | 7.1}

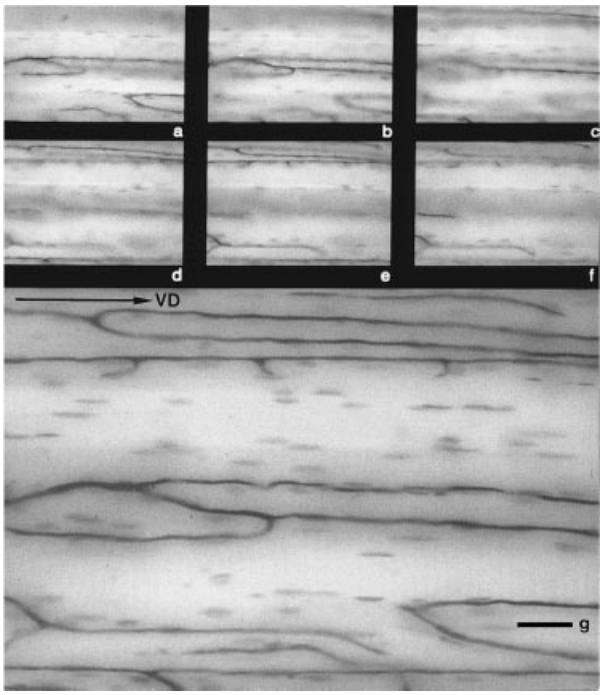

Fig. 3. (*a–f*) Sequence of 6 optical sections from a 50 μm thick section. The focal plane was moved down along the z-axis; the optical sections displayed were 5 μm apart, as read in the microcator. (*g*) Total projection of the preceding images. VD, vertical direction, see Fig. 1*a*. Bar, 25 μm.

Table 1. *Estimation of total capillary length with the fractionator design illustrated in Fig. 1*

Slab no.	No. quadrats	*I*(cap)	Slab no.	No. quadrats	*I*(cap)
1	68	932	2	125	2227
3	157	2376	4	155	2598
5	121	1951	6	98	1316
7	8	80	—	—	—
Total	354	5339	—	378	6141
est *L*(cap), m	—	642	—	—	739

est $L = (642+739)/2 = 691$ m.
$\mathrm{CE}(\mathrm{est}\,L) \approx (1/\sqrt{3})\cdot|5339-6141|/(5339+6141) \approx 0.040$.
* All blocks, first sampling period $f_1 = 1$; every 10th section, $f_2 = 10$; every 64th quadrat, $f_3 = 64$; and half the section thickness, $f_4 = 2$). *I*(cap) = number of intersections counted between capillaries and cycloid test curves, est *L*(cap) = estimate of total capillary length, $\mathrm{CE}(\mathrm{est}\,L) = \mathrm{SE}(\mathrm{est}\,L)/\mathrm{est}\,L$, corresponding coefficient of error, predicted via Eq. (5).

from which we can take the following two subsamples:

$S1$: {1.1 3.1 3.3 5.2 7.1}
$S2$: {1.2 3.2 5.1 5.3}.

The list of the 8 blocks from the even numbered slices is

{2.1 2.2 2.3 | 4.1 4.2 4.3 | 6.1 6.2}

and, likewise, we can take the following two subsamples:

$S3$: {2.1 2.3 4.2 6.1}
$S4$: {2.2 4.1 4.3 6.2}.

Thus, with $f_1 = 2$ we have 4 ways to estimate *L*, namely via {$S1$, $S3$}, {$S1$, $S4$}, {$S2$, $S3$} and {$S2$, $S4$) and each of these 4 combinations has probability 1/4 to be used. The corresponding est *L*s are, respectively, 701, 664, 717 and 680 m, (Table 2). Logically the mean of the 4

Table 2. *Estimation of total capillary length and error prediction when subsampling every other block ($f_1 = 2$) with the remaining periods as in Table 1*

Slab no.	Block	No. quadrats	*I*(cap)	Slab no.	Block	No. quadrats	*I*(cap)
Subsample 1							
1	1.1	34	384	2	2.1	45	762
3	3.1	52	853	—	2.3	5	89
	3.3	30	493	4	4.2	66	1399
5	5.2	46	791	6	6.1	51	975
7	7.1	8	80	—	—	—	—
Total	—	170	2601	—	—	167	3225
est *L*(cap), m	—	—	626	—	—	—	776
			est $L = 701$ m, $\mathrm{CE}(\mathrm{est}\,L) \approx 0.062$				
Subsample 2							
1	1.1	34	384	2	2.2	75	1376
3	3.1	52	853	4	4.1	59	647
	3.3	30	493	—	4.3	30	552
5	5.2	46	791	6	6.2	47	341
7	7.1	8	80	—	—	—	—
Total	—	170	2601	—	—	211	2916
est *L*(cap), m	—	—	626	—	—	—	702
			est $L = 664$ m, $\mathrm{CE}(\mathrm{est}\,L) \approx 0.033$				
Subsample 3							
1	1.2	34	548	2	2.1	45	762
3	3.2	75	1030	—	2.3	5	89
5	5.1	37	561	4	4.2	66	1399
	5.3	38	599	6	6.1	51	975
Total	—	184	2738	—	—	167	3225
est *L*(cap), m	—	—	659	—	—	—	776
			est $L = 717$ m, $\mathrm{CE}(\mathrm{est}\,L) \approx 0.047$				
Subsample 4							
1	1.2	34	548	2	2.2	75	1376
3	3.2	75	1030	4	4.1	59	647
5	5.1	37	561	—	4.3	30	552
	5.3	38	599	6	6.2	47	341
Total	—	184	2738	—	—	211	2916
est *L*(cap), m	—	—	659	—	—	—	702
			est $L = 680$ m, $\mathrm{CE}(\mathrm{est}\,L) \approx 0.018$				

* We consider the 4 possible subsamples from the original material (see text, *Assessment of precision*). To predict the error of this design we apply, in turn, Eq. (5) to each combination, and then Eq. (7).

estimates (691 m) coincides with the estimate obtained with all blocks (Eq. (6)), which illustrates unbiasedness. The corresponding CEs obtained via Eq. (5) are 6.2, 3.3, 4.7 and 1.8 %, respectively. The average CE has to be computed through the corresponding CE²s, namely:

$$\mathrm{CE}(\mathrm{est}\,L) \approx [(6.2^2+3.3^2+4.7^2+1.8^2)/4]^{1/2} \approx 4.3\,\%. \quad (7)$$

This result is relevant: it means that halving the workload at the first stage implies a negligible decrease in precision (from 4.0 % to 4.3 % CE) in this example.

All blocks ($f_1 = 1$), but every 40th section ($f_2 = 40$), and the remaining periods unchanged

From the available sections (which were 1/10th of the total) we take only every 4th (namely 1/40th of the total). We can do this in 4 different ways for each of the odd and even numbered slices, which makes a total of $4 \times 4 = 16$ combinations. We applied Eq. (5) to each combination, and the average CE, computed in a manner analogous to Eq. (7) was $\mathrm{CE}(\mathrm{est}\,L) \approx$ 4.7 %. The loss in precision is not large either, and we have reduced the workload by a factor of 4.

Every other block ($f_1 = 2$), every 40th section ($f_2 = 40$), and the remaining periods unchanged

This means a reduction in the workload by a factor of 8 with respect to the original design. Now we have 64 combinations in total, which yielded an average $\mathrm{CE}(\mathrm{est}\,L) \approx 6.2\,\%$, tolerable for designs in which the biological variation of the true L(cap) among animals is 6 % or more.

Every other block ($f_1 = 2$), every 40th section ($f_2 = 40$), every 256th quadrat ($f_3 = 256$), and remaining period $f_4 = 2$ unchanged

This means a further reduction by a factor of 4 with respect to the preceding design, namely 1/32 times the initial workload. There are 1024 combinations, with an average $\mathrm{CE}(\mathrm{est}\,L) \approx 7.4\,\%$, still moderate for many designs.

DISCUSSION

The fractionator/vertical slices design proposed in this paper seems to be a promising method to estimate total capillary length, because it enjoys the following advantages.

1. It is unbiased irrespective of capillary shape and degree of anisotropy. In this sense, it may replace with advantage alternative methods which require assumptions about the pattern of anisotropy (Mathieu et al. 1983; Mattfeldt & Mall, 1984; Cruz-Orive et al. 1985), because these assumptions are neither warranted in all cases, nor easy to check.

2. It is highly precise for a moderate workload, namely highly efficient. In the preceding subsection we have demonstrated that a reduction in the workload by a factor of 32 causes the CE to go up from 4.0 % to 7.4 %. Suppose that we are interested in estimating the mean of a group of animals from a sample of n animals. The impact that the mean $\mathrm{CE}(\mathrm{est}\,L) \approx 7.4\,\%$ within each animal has on the estimate of the group mean is $7.4/\sqrt{n}\,\%$. For instance, if $n = 9$ animals, the impact of the CE due to our design would be $7.4/\sqrt{9} \approx 2.5\,\%$. If we were content with a 5 % total error for the group mean estimate, the impact of the design error would be $2.5^2/5^2 = 1/4$ of the total error, and the remaining 3/4 would be due only to the biological variation among animals.

A further way to improve efficiency would be to reduce the cycloid length per unit test area, which was too high in the design described here. Let us suppose that we accept as reasonable a design with $f_1 = 2, f_2 = 50, f_3 = 100, f_4 = 2$. With this design the expected CE would probably be lower than 7 %, and note that here we would be looking at only a 1/20000th of the whole specimen, which gives an idea of the great efficiency of the fractionator. With our initial design we looked at $1/(1 \times 10 \times 64 \times 2) = 1/1280$th of the muscle (namely about 16 times more workload), and there we counted 11480 intersections. For the new design the expected total number of intersections would be about $11480/16 = 718$, which could still be halved without a significant loss in precision. To achieve this it would suffice to double the ratio a/l, i.e. from 23.5 to 40–50 μm.

3. Our design could in principle be applied to estimate feature length in quite different contexts, e.g. in neuroscience to estimate dendrite lengths. Here many of the recommendations given for instance in Cruz-Orive & Howard (1991), Howard et al. (1992, 1993) or Roberts & Cruz-Orive (1993) could be incorporated.

Additional recommendations on the use of the method are the following:

1. With the fractionator, tissue shrinkage is not important if the target parameter is dimensionless, e.g. particle number (Mayhew, 1988; Pakkenberg & Gundersen, 1988; Nairn et al. 1989; Geiser et al. 1990; West et al. 1991, 1996). In this case paraffin embedding does not induce any bias, which is an important advantage (Nyengaard & Bendtsen, 1990; Ogbuihi & Cruz-Orive, 1990) In our study the target parameter has length dimension and therefore tissue shrinkage

has to be minimised as much as possible; for this reason we recommend plastic embedding.

2. The initial splitting of the muscle into slabs does not need to be performed with a random start to preserve unbiasedness. In the fractionator, the splitting procedures may be arbitrary, i.e. nonrandom; only the successive subsampling procedures have to be strictly systematic with a random start from each collection of available pieces. Note also that a random start may produce too small slabs at either end of the muscle, which would preclude the cutting of proper slices or blocks there. Notwithstanding this, it must be pointed out that formula (5) was originally derived under the assumption that the initial slicing was performed with a random start.

3. Unlike the periods f_1, f_2, f_3 which, as we have seen, allow a flexible choice, the nominal section thickness (50 μm here) and the effective one (25 μm, which implies $f_4 = 2$) have to be chosen to optimise the identifiability of capillaries by optical scanning. Thus, in principle, these quantities do not allow much freedom of choice; they will depend upon feature length density, quality of the staining and of the embedding medium, etc.

4. The quadrat size depends on the magnification used, which should be the smallest possible which enables us to observe the capillaries unambiguously. Thus to change f_3 we are allowed to change the distance between quadrats, but not their size.

5. Whenever the capillaries, dendrites, etc. appear as strips after projection, with 2 clear boundaries, it is recommended to count intersections between the cycloids and these 2 boundaries separately, and then divide the global count by 2 before inserting it into the right hand side of Eq. (6) (Cruz-Orive & Howard, 1991; Roberts et al. 1991). Here we did not have to do this because the required magnification did not have to be large, and the capillaries appeared as thin curves after projection.

6. We do not recommend subsampling at the slab stage; all the slabs should be retained and split into primary vertical slices (called 'blocks' in this paper) which may already be subsampled with $f_1 = 2$, possibly 3.

ACKNOWLEDGEMENTS

The authors are grateful to R. Luque-Barona and E. Tarradas-Merino for their technical and photographic assistance. E. Artacho-Pérula acknowledges support from the Junta de Andalucía to visit the Department of Stereology, Institute of Anatomy, University of Berne, and L. M. Cruz-Orive acknowledges support of the Dirección General de Enseñanza Superior (DGES), Project No. PM97-0043.

REFERENCES

APPELL HJ (1980) Morphological studies on skeletal muscle capillaries under conditions of high altitude training. *International Journal of Sports Medicine* **1**, 103–109.

AQUIN L, BANCHERO N (1981) The cytoarchitecture and capillary supply in the skeletal muscle of growing dogs. *Journal of Anatomy* **132**, 341–356.

ARTACHO-PÉRULA E, ROLDÁN-VILLALOBOS R (1995*a*) Estimation of capillary length density in skeletal muscle by unbiased stereological methods. 1. Use of vertical slices of known thickness. *Anatomical Record* **241**, 337–344.

ARTACHO-PÉRULA E, ROLDÁN-VILLALOBOS R (1995*b*) Estimation of capillary length density in skeletal muscle by unbiased stereological methods. 2. Use of vertical slices of unknown thickness. *Anatomical Record* **241**, 345–352.

ARTACHO-PÉRULA E, ROLDÁN-VILLALOBOS R, VAAMONDE-LEMOS R (1990) Quantitative study of the microvascular pattern in tourniquet-induced muscular ischemia. *Analytical and Quantitative Cytology and Histology* **12**, 139–145.

ARTACHO-PÉRULA E, ROLDÁN-VILLALOBOS R, VAAMONDE-LEMOS R (1991) Capillary and fiber size interrelationships in regenerating soleus muscle after ischemia: A quantitative study. *Acta Anatomica* **142**, 70–76.

BADDELEY AJ, GUNDERSEN HJG, CRUZ-ORIVE LM (1986) Estimation of surface area from vertical sections. *Journal of Microscopy* **142**, 259–276.

BATRA S, KÖNIG ME, CRUZ-ORIVE LM (1995) Unbiased estimation of capillary length from vertical slices. *Journal of Microscopy* **178**, 152–159.

CRUZ-ORIVE LM (1990) On the empirical variance of the fractionator estimate. *Journal of Microscopy* **160**, 89–95.

CRUZ-ORIVE LM (1994) Toward a more objective biology. *Neurobiology of Aging* **15**, 377–378.

CRUZ-ORIVE LM (1997) Stereology of single objects. *Journal of Microscopy* **186**, 93–107.

CRUZ-ORIVE LM, HOPPELER H, MATHIEU O, WEIBEL ER (1985) Stereological analysis of anisotropic structures using directional statistics. *Applied Statistics* **34**, 14–32.

CRUZ-ORIVE LM, HOWARD CV (1991) Estimating the length of a bounded curve in three dimensions using total vertical projections. *Journal of Microscopy* **163**, 101–113.

GEISER M, CRUZ-ORIVE LM, IM HOF V, GEHR P (1990) Assessment of particle retention and clearance in the intrapulmonary conducting airways of hamster lungs with the fractionator. *Journal of Microscopy* **160**, 75–88.

GOKHALE AM (1990) Unbiased estimation of curve length in 3-D using vertical slices. *Journal of Microscopy* **159**, 133–141.

GUNDERSEN HJG (1986) Stereology of arbitrary particles. A review of unbiased number and size estimators and the presentation of some new ones, in memory of William R. Thompson. *Journal of Microscopy* **143**, 3–45.

GUNDERSEN HJG, ØSTERBY R (1981) Optimizing sampling efficiency of stereological studies in biology: or 'Do more less well!'. *Journal of Microscopy* **121**, 65–73.

HOPPELER H (1984) Morphometry of skeletal muscle capillaries. *Progress in Applied Microcirculation* **5**, 33–43.

HOPPELER H, MATHIEU O, WEIBEL ER, KRAUER R, LINDSTEDT SL, TAYLOR CR (1981) Design of the mammalian respiratory system. VIII. Capillaries in skeletal muscles. *Respiration Physiology* **44**, 129–150.

HOWARD CV, REED MG (1998) *Unbiased Stereology. Three-Dimensional Measurement in Microscopy*. Oxford: Bios.

HOWARD CV, CRUZ-ORIVE LM, YAEGASHI H (1992) Estimating neuron dendritic length in 3D from total vertical

projections and from vertical slices. *Acta Neurologica Scandinavica* **137**, 14–19.

HOWARD CV, JOLLEYS G, STACEY D, FOWLER A, WALLÉN P, BROWNE MA (1993) Measurement of total neuronal volume, surface area, and dendritic length following intracellular physiological recording. *Neuroprotocols* **2**, 113–120.

KANO Y, SHIMEGI S, MASUDA K, OHMORI H, KATSUTA S (1997) Morphological adaptation of capillary network in compensatory hypertrophied rat plantaris muscle. *European Journal of Applied Physiology and Occupational Physiology* **75**, 97–101.

KROGH A (1919) The number and distribution of capillaries in muscles with calculation of the oxygen pressure head necessary for supplying the tissue. *Journal of Physiology* **52**, 409–415.

LARSEN JO, GUNDERSEN HJG, NIELSEN J (1998) Global spatial sampling with isotropic virtual planes: estimators of length density and total length in thick, arbitrarily orientated sections. *Journal of Microscopy* **191**, 238–248.

MATHIEU-COSTELLO O (1993) Comparative aspects of muscle capillary supply. *Annual Review of Physiology* **55**, 503–525.

MATHIEU O, CRUZ-ORIVE LM, HOPPELER H, WEIBEL ER (1983) Estimating length density and quantifying anisotropy in skeletal muscle capillaries. *Journal of Microscopy* **131**, 131–146.

MATTFELDT T, MALL G (1984) Estimation of length and surface of anisotropic capillaries. *Journal of Microscopy* **135**, 181–190.

MAYHEW TM (1988) An efficient sampling scheme for estimating fibre number from nerve cross sections: the fractionator. *Journal of Anatomy* **157**, 127–134.

McMILLAN PJ, ARCHAMBEAU JO, GOKHALE AM, ARCHAMBEAU MH, OEY M (1994) Morphometric and stereologic analysis of cerebral cortical microvessels using optical sections and thin slices. *Acta Stereologica* **13**, 33–38.

MYRHAGE R (1977) Microvascular supply of skeletal muscle fibers. A microangiographic, histochemical and intravital microscopic study of hind limb muscles in the rat, rabbit and cat. *Acta Orthopaedica Scandinavica* **168**, 1–46.

NAIRN JG, BEDI KS, MAYHEW TM, CAMPBELL LF (1989) On the number of Purkinje cells in the human cerebellum: unbiased estimates obtained by using the 'fractionator'. *Journal of Comparative Neurology* **290**, 527–532.

NYENGAARD JR, BENDTSEN TF (1990) A practical method to count the number of glomeruli in the kidney as exemplified in various animal species. *Acta Stereologica* **9**, 243–258.

OGBUIHI S, CRUZ-ORIVE LM (1990) Estimating the total number of lymphatic valves in infant lungs with the fractionator. *Journal of Microscopy* **158**, 19–30.

PAKKENBERG B, GUNDERSEN HJG (1988) Total number of neurons and glial cells in human brain nuclei estimated by the disector and the fractionator. *Journal of Microscopy* **150**, 1–20.

PLYLEY MJ, GROOM AC (1975) Geometrical distribution of capillaries in mammalian striated muscle. *American Journal of Physiology* **228**, 1376–1383.

PLYLEY MJ, SUTHERLAND GJ, GROOM AC (1976) Geometry of the capillary network in skeletal muscle. *Microvascular Research* **11**, 161–173.

PLYLEY MJ, OLMSTEAD BJ, NOBLE EG (1998) Time-course of changes in capillarization in hypertrophied rat plantaris muscle. *Journal of Applied Physiology* **84**, 902–907.

POOLE DC, MATHIEU-COSTELLO O (1989) Skeletal muscle capillary geometry: adaptation to chronic hypoxia. *Respiration Physiology* **77**, 21–29.

RIPOLL E, SILLAU AH, BANCHERO N (1979) Changes in the capillarity of skeletal muscle in the growing rat. *Pflügers Archiv* **380**, 153–158.

ROBERTS N, HOWARD CV, CRUZ-ORIVE LM, EDWARDS RHT (1991) The application of total vertical projections for the unbiased estimation of the length of blood vessels and other structures by magnetic resonance imaging. *Magnetic Resonance Imaging* **9**, 917–925.

ROBERTS N, CRUZ-ORIVE LM (1993) Spatial distribution of curve length: concept and estimation. *Journal of Microscopy* **172**, 23–29.

SILLAU AH, BANCHERO N (1997) Effects of hypoxia on capillary density and fiber composition in rat skeletal muscle. *Pflügers Archiv* **370**, 227–232.

SNYDER GK (1995) Capillary growth in chick skeletal muscle with normal maturation and hypertrophy. *Respiration Physiology* **102**, 293–301.

WEST MJ, SLOMIANKA L, GUNDERSEN HJG (1991) Unbiased stereological estimation of the total number of neurons in the subdivisions of the rat hippocampus using the optical fractionator. *Anatomical Record* **231**, 482–497.

WEST MJ, ØSTERGAARD K, ANDREASSEN OA, FINSEN B (1996) Estimation of the number of somatostatin neurons in the striatum: an in situ hybridization study using the optical fractionator method. *Journal of Comparative Neurology* **370**, 11–22.